Conformational selection guides β-arrestin recruitment at a biased G protein–coupled receptor

Kleist, Andrew B.; Jenjak, Shawn; Sente, Andrija; Laskowski, Lauren J.; Szpakowska, Martyna; Calkins, Maggie M.; Anderson, Emilie I.; McNally, Lisa M.; Heukers, Raimond; Bobkov, Vladimir; Peterson, Francis C.; Thomas, Monica A.; Chevigné, Andy; Smit, Martine J.; McCorvy, John D.; Babu, M. Madan; Volkman, Brian F.

published in
Science
2022

DOI (link to publisher)
10.1126/science.abj4922

document version
Publisher's PDF, also known as Version of record

STRUCTURAL BIOLOGY

Conformational selection guides β-arrestin recruitment at a biased G protein–coupled receptor

Andrew B. Kleist[1,2]†‡, Shawn Jenjak[1]†, Andrija Sente[3], Lauren J. Laskowski[4], Martyna Szpakowska[5], Maggie M. Calkins[4], Emilie I. Anderson[4], Lisa M. McNally[4], Raimond Heukers[6]§, Vladimir Bobkov[6], Francis C. Peterson[1], Monica A. Thomas[1,2]¶, Andy Chevigné[5], Martine J. Smit[6], John D. McCorvy[4], M. Madan Babu[7,8], Brian F. Volkman[1]*

G protein–coupled receptors (GPCRs) recruit β-arrestins to coordinate diverse cellular processes, but the structural dynamics driving this process are poorly understood. Atypical chemokine receptors (ACKRs) are intrinsically biased GPCRs that engage β-arrestins but not G proteins, making them a model system for investigating the structural basis of β-arrestin recruitment. Here, we performed nuclear magnetic resonance (NMR) experiments on $^{13}CH_3$-ε–methionine–labeled ACKR3, revealing that β-arrestin recruitment is associated with conformational exchange at key regions of the extracellular ligand-binding pocket and intracellular β-arrestin–coupling region. NMR studies of ACKR3 mutants defective in β-arrestin recruitment identified an allosteric hub in the receptor core that coordinates transitions among heterogeneously populated and selected conformational states. Our data suggest that conformational selection guides β-arrestin recruitment by tuning receptor dynamics at intracellular and extracellular regions.

Once thought of as G protein–coupled receptor (GPCR) off-switches, β-arrestins are now known to coordinate diverse, G protein–independent signaling responses (*1*). In a phenomenon called biased signaling,some GPCR ligands (biased ligands) preferentially recruit β-arrestins or G proteins (*2*). Because they select one pathway, and therefore a specific functional outcome, biased ligands have demonstrated advantages over conventional ligands in preclinical (*3*–*5*) and clinical (*6*, *7*) testing. More than 30% of US Food & Drug Administration–approved drugs target GPCRs (*8*), so understanding the mechanistic basis by which GPCRs recruit β-arrestins has important implications for drug development.

Recent GPCR–β-arrestin structures (*9*–*11*) and biophysical studies of β-arrestin–biased ligands (*12*–*14*) provide mechanistic insights into β-arrestin recruitment. For instance, structural comparisons of GPCRs bound to antagonists and β-arrestin–biased ligands suggest that ligand-specific conformational changes govern β-arrestin recruitment (*12*, *13*). Despite this progress, how ligand-binding pocket changes are transmitted to the β-arrestin interface remains poorly understood. Other findings have complicated our understanding of β-arrestin recruitment by GPCRs. The identification of multiple, distinct β-arrestin–recruiting GPCR conformations suggests there may be multiple conformational solutions to β-arrestin recruitment (*15*), but raises the question of how such different conformations could elicit similar outcomes. Conversely, nearly identical conformations of β-arrestin– and G protein–bound GPCRs (*9*–*11*) suggest that conformational changes alone might not account for β-arrestin recruitment. Finally, some studies of β-arrestin recruitment use ligands that provoke residual signaling at G proteins (*16*), making it challenging to isolate the specific molecular changes leading to β-arrestin recruitment.

Given these complexities, studies of β-arrestin recruitment could benefit from functionally decoupled receptors that exclusively recruit β-arrestin. Atypical chemokine receptors (ACKRs) represent one such naturally occurring system. ACKR3 is an intrinsically β-arrestin–biased GPCR that recruits β-arrestin but does not activate G protein (Fig. 1A) (*17*). Here, we performed nuclear magnetic resonance (NMR) studies of ACKR3, showing that β-arrestin recruitment at an intrinsically biased GPCR is guided by tuning its conformational equilibrium.

RESULTS

In agreement with prior studies, ACKR3 recruits β-arrestin but does not activate G protein signaling (Fig. 1, A and B; fig. S1A; and table S1). To investigate the mechanisms underlying β-arrestin recruitment at ACKR3, we first measured β-arrestin-2 recruitment in response to a panel of ACKR3 agonists, including the endogenous chemokine CXCL12 [median effective concentration (EC_{50}) = 0.75 nM] (*18*), the small molecule CCX777 (EC_{50} = 0.95 nM; maximum effect (E_{max}, % of CXCL12) = 75 ± 2%] (*19*), and a recently described peptide LIH383 (EC_{50} = 4.8 nM; E_{max} = 83 ± 1%) (Fig. 1C) (*20*). We also identified a potent, extracellular-targeting, ACKR3-competitive antagonist nanobody called VUN701 [median inhibitory concentration (IC_{50}) = 1.47 μM] using nanobody phage display (Fig. 1C; fig. S1, B to F; and materials and methods). These four ligands display a range of activities for β-arrestin-2 recruitment, allowing us to sample inactive (i.e., VUN701-bound) and active (i.e., CCX777-, LIH383-, and CXCL12-bound) β-arrestin–recruiting states of ACKR3 (Fig. 1D).

NMR spectroscopy allows simultaneous characterization of receptor conformation at multiple sites (*21*). We previously purified $^{13}CH_3$-ε-Met–labeled, ACKR3-bound CCX777 in lauryl maltose neopentyl glycol/cholesteryl hemisuccinate (MNG/CHS) micelles for NMR studies (*22*), and we used this method for other ACKR3-ligand complexes here (Fig. 1E, figs. S2 and S3, and materials and methods). As with other GPCRs, copurification with ligands was necessary to produce sufficient quantities of ACKR3 for NMR studies (*23*). Structural homology modeling of ACKR3 (fig. S4 and materials and methods) demonstrates eight native Met residues (excluding the N-terminal Met) distributed in ACKR3's tertiary structure for NMR labeling. NMR labels serve as sensitive probes reporting on regional changes in GPCR conformation and dynamics (*24*, *25*). In this setting, $Met212^{5x39}$ and $Met138^{3x46}$ [where the superscripts indicate GPCRdb nomenclature (*26*)] are well positioned to report on conformational changes associated with β-arrestin recruitment at ACKR3 because they are located in key regions of the ligand-binding pocket (*27*, *28*) and intracellular effector binding interface (*29*), respectively.

Ligand interactions with TM5 play key roles in GPCR activation (*27*, *30*), but how conformational changes in TM5 lead to β-arrestin recruitment is unclear. NMR spectra for the four ligand-bound states show chemical shift perturbations (CSPs) for the $Met212^{5x39}$ peak, which remains colinear along the ^1H axis but variable along the ^{13}C axis (Fig. 2, A and B). This indicates that ACKR3 exists along a two-state equilibrium, with the peaks at either extreme defining the conformational end points (*31*). In the CCX777-bound state, downfield peak positions [~18.2 to 19 parts per million (p.p.m.)] indicate that $^{13}CH_3$ is in a *trans* rotamer (end point 1), whereas in the CXCL12- and LIH383-bound states, upfield peak positions

[1]Department of Biochemistry, Medical College of Wisconsin, Milwaukee, WI 53226, USA. [2]Medical Scientist Training Program, Medical College of Wisconsin, Milwaukee, WI 53226, USA. [3]MRC Laboratory of Molecular Biology, Cambridge CB2 0QH, UK. [4]Department of Cell Biology, Neurobiology, and Anatomy, Medical College of Wisconsin, Milwaukee, WI 53226, USA. [5]Immuno-Pharmacology and Interactomics, Department of Infection and Immunity, Luxembourg Institute of Health (LIH), L-4354 Esch-sur-Alzette, Luxembourg. [6]Amsterdam Institute for Molecular and Life Sciences, Division of Medicinal Chemistry, Faculty of Sciences, Vrije Universiteit, 1081 HZ Amsterdam, Netherlands. [7]Department of Structural Biology, St. Jude Children's Research Hospital, Memphis, TN 38105, USA. [8]Center for Data Driven Discovery, St. Jude Children's Research Hospital, Memphis, TN 38105, USA.
*Corresponding author. Email: bvolkman@mcw.edu
†These authors contributed equally to this work. ‡Present address: Harriet Lane Pediatric Residency Program, Johns Hopkins Children's Center, Baltimore, MD 21287, USA. §Present address: QVQ Holding BV, 3584 CL Utrecht, Netherlands. ¶Present address: Department of Anesthesiology and Critical Care Medicine, Johns Hopkins Medicine, Baltimore, MD 21287, USA.

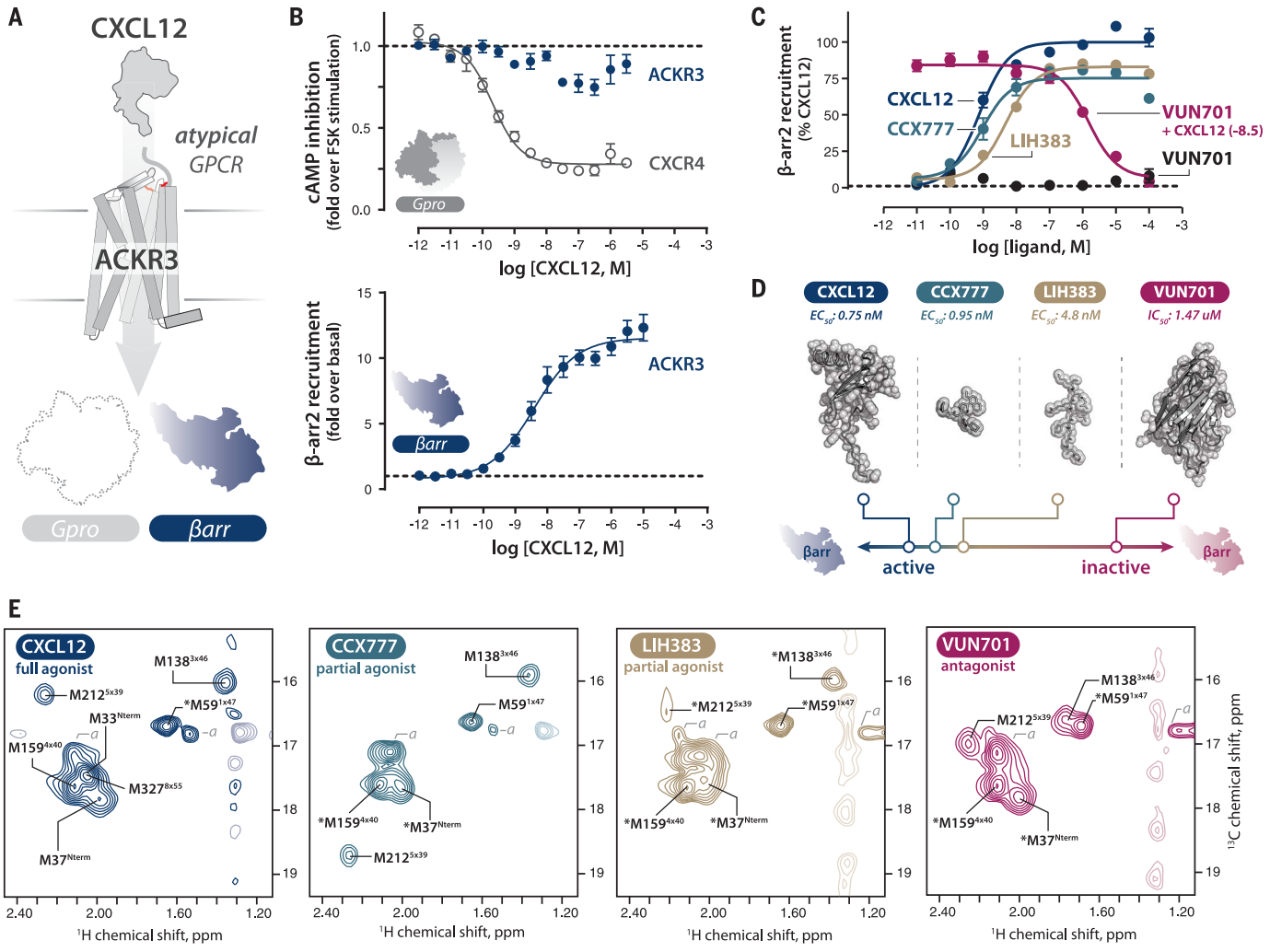

Fig. 1. β-arrestin–biased signaling at ACKR3 and structural characterization by NMR. (**A**) CXCL12 activates β-arrestin but not G protein at ACKR3. (**B**) CXCL12-mediated cAMP inhibition of CXCR4 (positive control) and ACKR3 as shown by Glosensor assay (EC_{50} = 0.21 nM, CXCR4) (top). CXCL12-mediated β-arrestin-2 recruitment to ACKR3 as shown by Tango assay (EC_{50} = 3.9 nM, ACKR3) (bottom). N = 3 in triplicate in both assays. Error bars indicate SEM. (**C**) β-arrestin recruitment to ACKR3 as shown by Nano-BiT assay. VUN701 dose response alone could not be fit (black circles). Purple circles reflect VUN701 dose response with CXCL12 at 3.2 nM . See text and table S1 for EC_{50} and E_{max}. All conditions, N = 3 in duplicate. Error bars indicate SEM. (**D**) Summary of ligand potency at β-arrestin recruitment. Structures are not to scale. CXCL12 PDB: 2KEC; nanobody from PDB 6KNM used to represent VUN701, and LIH383 and CCX777 were modeled in PyMol. LIH383 sequence is FGGFMRRK (*20*). The chemical structure of CCX777 is shown in (*19*). (**E**) ^{1}H-^{13}C heteronuclear single quantum coherence NMR spectra of WT-ACKR3 with various ligands at 310 K. Assigned Met residues are labeled. Asterisk denotes inferred assignments from other ligand-bound states (see the materials and methods). Negative contour peaks are shown in semitransparency and dashed lines. Peaks marked "*a*" encompass natural abundance peaks from buffer and detergent components (see also figs. S2G and S3). All spectra are shown at the same contour except LIH383, which was lowered to represent $M212^{5x39}$.

(~16 to 16.5 p.p.m.) indicate that $^{13}CH_3$ is in a *gauche* rotamer (end point 2) (Fig. 2B and fig. S5, A and B) (*22*, *32*–*34*).

By contrast, in VUN701-bound ACKR3, the $Met212^{5x39}$ peak appears between the two end points at the random coil $^{13}CH_3$ position, indicating fast conformational exchange between *gauche* and *trans* rotamers in the inactive, β-arrestin–nonrecruiting state (Fig. 2B). Indeed, CSPs of $Met212^{5x39}$ from $^{13}CH_3$ random coil vary by ligand type (fig. S5A), suggesting that β-arrestin recruitment is associated with decreasing exchange among $Met212^{5x39}$ rotamers irrespective of which χ_3 rotameric state is selected. Antagonists such as VUN701 may fail to constrain the region sampled by $Met212^{5x39}$, preserving conformational heterogeneity (seen by increased exchange relative to the active state) and precluding TM5-binding pocket stabilization required for ACKR3 activation. Binding data show that Ala mutagenesis of $Met212^{5x39}$ similarly affects CXCL12 and VUN701, suggesting that NMR changes between inactive and active states likely represent functionally important regional conformational changes, as opposed to differences in direct ligand contacts at the probe residue (fig. S5, C to E, and table S1). Indeed, $Met212Ala^{5x39}$ has equivalent efficacy for β-arrestin recruitment as wild type (WT) (fig. S5F), indicating that $Met212^{5x39}$ reports on but does not itself mediate functional changes in the TM5 region.

Does this occur in other GPCRs? We identified all ligand-contacting residues among structures of (i) GPCRs bound to β-arrestin–biased ligands (or full-length β-arrestin; jointly called β-arresting–recruiting states) and (ii) inactive-state structures of the same GPCRs (fig. S6, A and B). Using contact network analysis (*29*, *35*), we found that ligands in β-arrestin–recruiting states make similar numbers of contacts with residues in TM5 but significantly

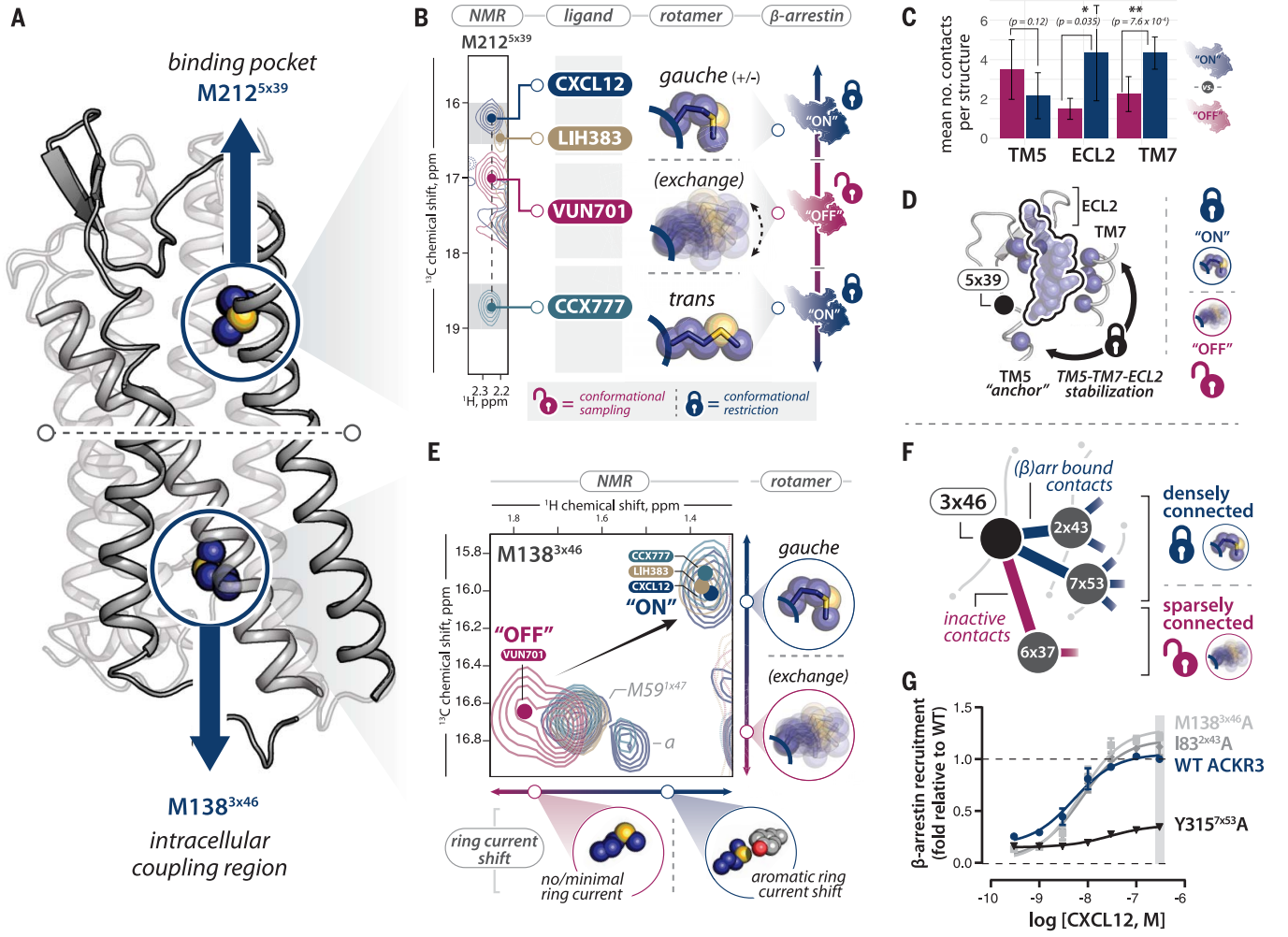

Fig. 2. Conformational changes in the ligand-binding pocket and intracellular region characterize the β-arrestin–recruiting state. (**A**) ACKR3 model depicting M212^{5x39} and M138^{3x46} probes. (**B**) Overlay of M212^{5x39} peaks from ligand-bound ACKR3 complexes at 310 K. The 16 to 16.5 and 18.5 to 19 p.p.m. peaks (^{13}C) correspond to *gauche* and *trans* rotameric states, respectively. Ligand-specific β-arrestin activity is depicted at right. Open and closed locks depict conformational sampling and restriction, respectively (bottom). (**C**) Ligand-residue interactions were compared between antagonist and β-arrestin–biased ligand-bound GPCRs (see the materials and methods). Shown is a comparison of the mean number of ligand contacts with TM5, ECL2, and TM7 residues. *P < 0.05; **P < 0.005, unpaired t test. (**D**) AT$_1$R contacts with the ligand TRV023 (β-arrestin–biased; black outline) in TM5, ECL2, and TM7 are shown as blue spheres (PDB 6OS1). The position of NMR probe 5x39 in AT$_1$R is shown. Stabilization of TM5-ECL2-TM7 by biased ligands is depicted as a lock (right). (**E**) Met138^{3x46} peaks in all four ligand-bound states. Upfield peak positions (^{1}H: ~1.3 p.p.m.) of M138^{3x46} among agonist-bound states supports ring-current shifts due to aromatic side chain interactions. Peaks are marked "*a*" as in Fig. 1. (**F**) 3x46 contact residues at 2x43 and 7x53 exclusively in active-state complexes and 6x37 exclusively in inactive-state complexes (see the materials and methods). (**G**) β-arrestin recruitment of WT ACKR3 versus Ala mutants of 3x46-contacting mutants by NanoBiT (N = 3). See also table S1.

more contacts with residues in ECL2 and TM7 than do antagonists (Fig. 2C). Thus, TM5 may anchor agonist interactions with ECL2 and TM7 (*27*, *36*), creating a tripartite lock involving the 5x39 region (Fig. 2D and fig. S6C), whereas antagonists fail to stabilize all three lock points (ECL2, TM5, and TM7) simultaneously.

Large-scale conformational changes underlying GPCR activation are driven by local rearrangements of residues at key positions in the GPCR structure (so-called microswitch residues (*37*). We next examined Met138^{3x46}, a microswitch residue in the β-arrestin–coupling region (Fig. 2A) (*29*). In the three agonist-bound states (CXCL12-, CCX777-, and LIH383-bound), the Met138^{3x46} NMR peak has nearly identical chemical shifts (Fig. 2E), indicating that all three agonists elicit a shared conformation of Met138^{3x46}. The upfield position (~1.3 p.p.m.) of Met138^{3x46} in the ^{1}H dimension likely reflects ring current shifts caused by proximity to an aromatic side chain (*33*, *38*, *39*). These data indicate that the agonist-specific conformations of Met212^{5x39} (i.e., *trans* versus *gauche*) in the TM5-binding pocket are funneled into a common conformation at the β-arrestin–coupling region sampled by M138^{3x46}.

By contrast, the inactive, VUN701-bound ACKR3 state is characterized by CSPs of the Met138^{3x46} peak in both ^{1}H and ^{13}C values (Fig. 2E), indicating diminished ring-current shift (^{1}H dimension), depletion of the *gauche* rotamer (^{13}C dimension), and more *gauche*/*trans* exchange (^{13}C dimension). As in the binding pocket, VUN701 causes the smallest CSP from random coil $^{13}CH_3$-ε-Met versus the three agonists, suggesting that agonists regulate β-arrestin recruitment by decreasing

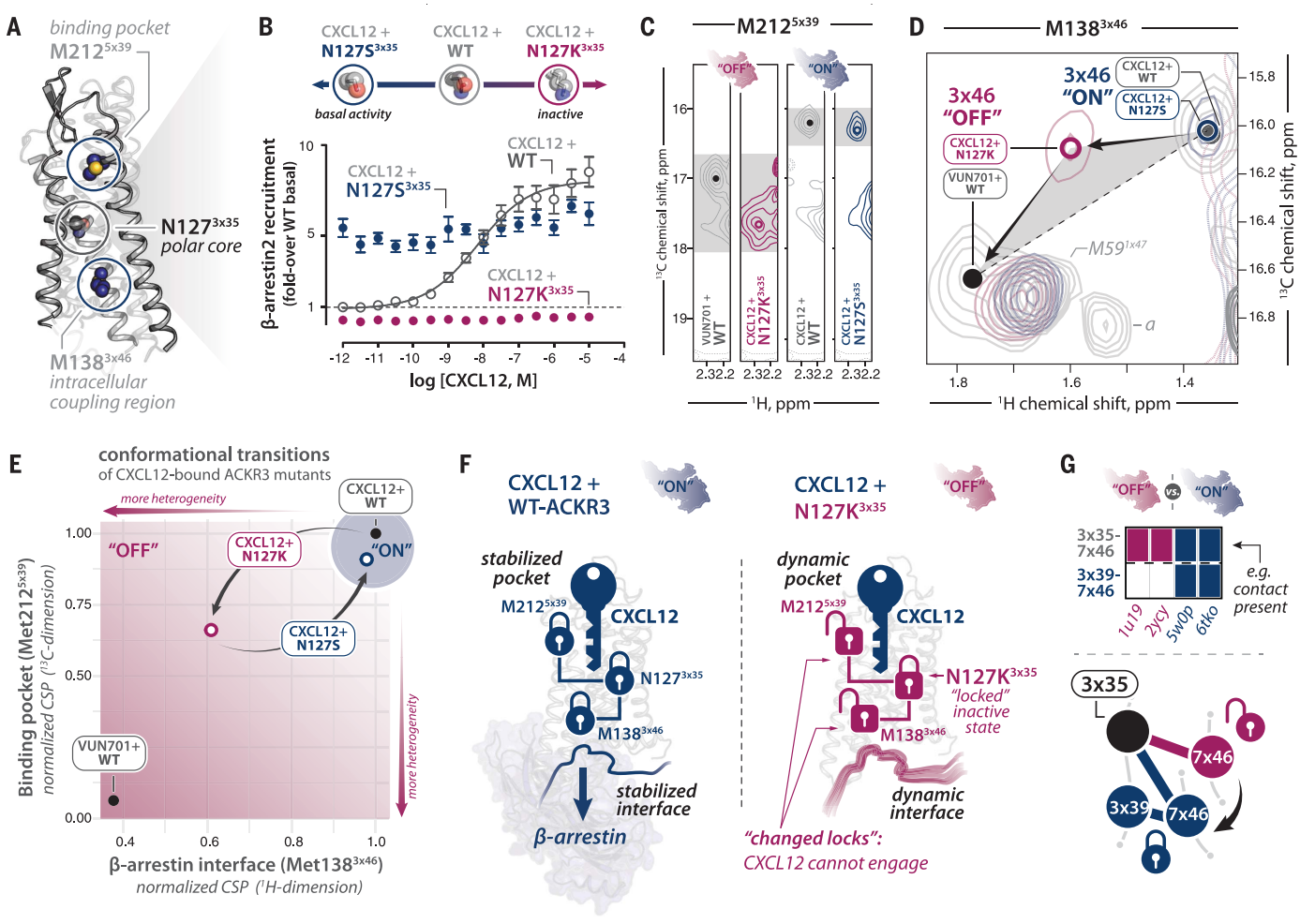

Fig. 3. Mutational inactivation of β-arrestin recruitment through the conserved polar network. (**A**) Position of Asn127^{3x35} in the ACKR3 model relative to Met212^{5x39} and Met138^{3x46}. (**B**) β-arrestin-2 recruitment with CXCL12 for the ACKR3 mutants Asn127Lys^{3x35} and Asn127Ser^{3x35} as shown by the Tango assay. All conditions, *N* = 3 in triplicate. Error bars indicate SEM. See also table S1. (**C**) Close-up view of ^{1}H-^{13}C-HSQC in the Met212^{5x39} region (right), highlighting VUN701-WT-ACKR3 (first panel), CXCL12-ACKR3 Asn127Lys^{3x35} (second panel), CXCL12-WT-ACKR3 (third panel), and CXCL12-ACKR3 Asn127Ser^{3x35} (fourth panel). (**D**) Overlay of ^{13}C-HSQC in the Met138^{3x46} region for WT-ACKR3-VUN701, ACKR3-Asn127Lys^{3x35}-CXCL12, ACKR3-Asn127Ser^{3x35}-CXCL12, and WT-ACKR3-CXCL12 complexes. A shaded triangle suggests peak noncolinearity. Peaks are marked "*a*" as in Fig. 1. See fig. S8A and legend for the Met138^{3x46} assignment method. (**E**) Normalized CSPs for Met212^{5x39} in the ^{13}C dimension (*y* axis) and Met138^{3x46} in the ^{1}H dimension (*x* axis) from random coil for Asn127^{3x35} mutants and CXCL12- and VUN701-bound WT-ACKR3. Arrows depict transitions among CXCL12-bound WT-ACKR3 and mutant ACKR3. (**F**) Depiction of differences between WT-ACKR3 and Asn127Lys^{3x35} in CXCL12-bound states. Despite being bound to CXCL12 (blue key), Asn127Lys^{3x35} locks ACKR3 in the inactive state, abrogating CXCL12's effects on the Met212^{5x39} and Met138^{3x46} probes. (**G**) Comparison of residue-residue interactions AT_1R–β-arrestin–biased ligand and AT1R-antagonist bound states (top) reveals the formation of a 3x39–7x46 interaction in the β-arrestin state (bottom).

conformational heterogeneity in this region of the β-arrestin–coupling region relative to the inactive state (fig. S7A).

What is the role of 3x46, a known microswitch involved in G protein activation (*29*), in β-arrestin recruitment among other GPCRs? We calculated all intramolecular, residue-residue interactions among structures of (i) β-arrestin-bound and (ii) inactive-state structures of GPCRs with resolved side chains (β_1AR and rhodopsin) (fig. S7, B and C), finding that 3x46 contacts 2x43 and 7x53 in β-arrestin-bound structures and 6x37 in inactive structures (Fig. 2F and fig. S7, D to F). Of note 7x53 is a highly conserved Tyr among class A GPCRs (*37*), and 7x53 and 6x37 have been shown to stabilize GPCRs in G protein signaling (7x53) and inactive states (6x37), respectively (*29*).

To investigate whether 3x46 and active-state contacts from GPCR-β–arrestin complexes (2x43 and 7x53) might play a role in β-arrestin recruitment to ACKR3, we tested Met138Ala^{3x46}, Ile84Ala^{2x43}, and Tyr315Ala^{7x53} mutants for β-arrestin recruitment (Fig. 2G and table S1). Although Met138Ala^{3x46} and Ile84Ala^{2x43} minimally affected ACKR3 function, Tyr315Ala^{7x53} almost completely abolished β-arrestin recruitment, demonstrating the essential role for this residue on ACKR3 activation. The close proximity of 3x46 to Tyr^{7x53} (Fig. 2F and fig. S7, D to F) and the pronounced ring current shift (^{1}H) of Met138^{3x46} (Fig. 2E) in active but not inactive states of ACKR3 suggest that Met138^{3x46} reports on dynamic alterations in Tyr315^{7x53} associated with β-arrestin recruitment (*33*, *38*, *39*). Active-state interactions between 3x46 and 7x53 may thus lock this region in place, decreasing local conformational heterogeneity and increasing the likelihood of β-arrestin engagement. Indeed, receptors contact the β-arrestin finger loop, a key structural region anchoring GPCR-β–arrestin interactions, directly at or in the vicinity of 3x46 and 7x53 in β_1AR- and rhodopsin-arrestin complexes (*11*, *40*). By contrast, a more heterogeneous

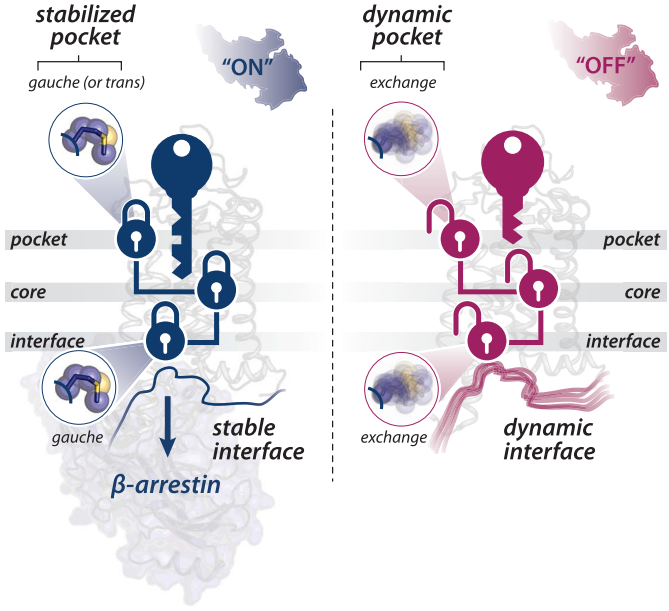

Fig. 4. Dynamic control of β-arrestin recruitment to ACKR3. Allosteric regulation of GPCR β-arrestin activation by coordinated transitions in conformational heterogeneity. Ligands constrain (agonists) or promote (antagonists) conformational heterogeneity by altering intermolecular (ligand-residue) and intramolecular (residue-residue) interactions throughout the GPCR structure.

inactive state (characterized by rotameric exchange and a diminished ring current shift at Met138^{3x46}) may reflect absent interactions with 7x53 and a lower propensity for β-arrestin engagement (Fig. 2F).

To what extent are dynamic changes in extracellular (Met212^{5x39}) and intracellular (Met138^{3x46}) probes allosterically linked through the receptor core during ACKR3 activation? Conserved polar core residues, including the residue Asn^{3x35} (*12*, *41*, *42*), coordinate a sodium ion (inactive state) and a water network (active state) to regulate GPCR activation and bias (Fig. 3A) (*42*). We investigated the effects of known inactivating and constitutively activating mutations of conserved polar core residue Asn127^{3x35} on ACKR3 activation. Consistent with prior results, the Asn127Lys^{3x35} mutation showed complete inactivity in β-arrestin recruitment (Fig. 3B), whereas Asn127Ser^{3x35} acts as a constitutively active mutant (Fig. 3B and table S1) (*43*).

How do Asn127^{3x35} mutants affect the conformation and stability of the binding pocket and intracellular probes as observed by NMR chemical shifts? In the context of CXCL12, the Asn127Lys^{3x35} mutation shifts the Met212^{5x39} peak downfield relative to its position in the WT-ACKR3 complex (Fig. 3C and fig. S8A), resembling the VUN701-bound state characterized by *trans*/*gauche* rotamer exchange at Met212^{5x39}. This reveals that the receptor core mutation exerts long-range, allosteric effects that enhance conformational exchange in the extracellular ligand-binding pocket. The Asn127Lys^{3x35} mutation shifts the Met138^{3x46} peak downfield in both the ^{1}H and ^{13}C values to an intermediate position between those in CXCL12- and VUN701-bound states (Fig. 3D). This peak is not colinear with CXCL12 and VUN701, suggesting the occupancy of a third, distinct conformation in this ACKR3 mutant. Although Met138^{3x46} in this mutant occupies a *gauche* rotamer (^{13}C: ~16.1 p.p.m.), its ^{1}H value is closer to that of VUN701-bound ACKR3, suggesting fewer local aromatic interactions resulting in a diminished ring current shift. We speculate that this downfield ^{1}H shift reflects increased conformational exchange between both *gauche* rotamers (i.e., + and −) in the mutant state, which would weaken interactions with an aromatic side chain compared with a single *gauche* rotamer (i.e., + or −) in the active state (fig. S8B). Regardless, pronounced downfield ^{1}H shifts and peak broadening of Met138^{3x46} in the CXCL12-bound, inactivating Asn127Lys^{3x35} mutant reveal that, as in the ligand-binding pocket, the conserved core mutation abrogates β-arrestin-2 recruitment by increasing conformational heterogeneity at a key position in the β-arrestin–coupling region (Fig. 3E). Thus, a single mutation in the receptor core, Asn127Lys^{3x35}, destabilizes ACKR3 at extracellular and intracellular sites, overriding the effects of CXCL12 to decrease conformational exchange present in WT ACKR3 (Fig. 3F).

In the CXCL12-bound, constitutively active Asn127Ser^{3x35} mutant receptor, Met212^{5x39} and Met138^{3x46} peaks overlay those in the CXCL12-WT-ACKR3 state (Fig. 3, C to E, and fig. S8A) despite this state's unresponsiveness to CXCL12, indicating that the activating mutation promotes conformational homogeneity (no rotameric exchange) extracellularly and intracellularly, even as it decouples allosteric transmembrane communication. By contrast, VUN701 decreases the elevated basal β-arrestin recruitment of ACKR3 Asn127Ser^{3x35}, suggesting that it acts as an inverse agonist at this mutant (fig. S8C and table S1). As shown by NMR, the VUN701-bound Asn127Ser^{3x35} mutant reverts to the inactive (i.e., *trans*/*gauche* interconverting) state at Met212^{5x39}, and the Met138^{3x46} peak is diminished, suggesting transition to a more dynamic state at both probes (fig. S8, D to G).

Among analyzed GPCR structures (i.e., those bound to β-arrestin or β-arrestin–biased ligands), AT$_1$R is most closely related to ACKR3 and is the only one that shares Asn^{3x35}. Calculation of intramolecular, residue-residue interactions of AT$_1$R bound to antagonists and β-arrestin–biased agonists revealed that whereas 3x35 interacts with 7x46, a key residue for β-arrestin recruitment (*12*) in both states, 7x46 interacts with 3x39, which is also involved in β-arrestin recruitment (*12*), only in the active state (Fig. 3G). This rearrangement in turn shifts the register of TM3 and TM7 relative to one another in the region above 3x46 and 7x53 (Fig. 3G), suggesting a mechanism by which 3x35 mutations in ACKR3 might be transmitted to the β-arrestin–coupling region as observed at the intracellular probe Met138^{3x46}. In effect, Asn^{3x35} mutations in ACKR3 may function by promoting (active) or disrupting (inactive) 3x39–7x46 interactions, resulting in decreased (active) or increased (inactive) conformational exchange at the intracellular probe.

DISCUSSION

Some studies have identified distinct conformational changes associated with β-arrestin recruitment (*12*, *13*), but others have shown multiple β-arrestin competent conformations (*14*). How can β-arrestin be both sensitive to and tolerant of GPCR conformational changes?

The results presented here help to reconcile this apparent contradiction by revealing that whereas β-arrestin is tolerant of diverse GPCR conformations in some parts of the receptor, it may have more stringent conformational requirements in other parts. At TM5 of the ligand-binding pocket, we found that multiple conformational solutions (*15*) are compatible with β-arrestin recruitment. These multiple-binding-pocket conformations are funneled into a single active conformation as monitored at the intracellular probe Met138^{3x46}. NMR and structural evidence for active-state interactions between 3x46 and 7x53 suggest that the stringent intracellular conformational requirements comprise the intracellular regions of TM3 and TM7. Indeed, although studies of AT$_1$R bound to multiple β-arrestin agonists have revealed diverse intracellular conformations, most variation was in TM5 and TM6, with only modest variation in TM7 (*14*).

Conformational control, although important, may not fully account for β-arrestin recruitment. The observation that intracellular and

extracellular probes both transition between conformational heterogeneity (inactive) and homogeneity (active) suggests that β-arrestin recruitment is governed in part by tuning the conformational spectrum sampled by the receptor. The regulation of β-arrestin recruitment in this manner could help to explain the apparent agnosticism of β-arrestin for specific GPCR conformations (*14*): Alteration of receptor stability in key regions may tune a GPCR's ability to couple β-arrestin irrespective of conformation (e.g., at $Met212^{5x39}$). Likewise, globally different GPCR conformations may be similarly tuned to couple β-arrestins by decreasing conformational heterogeneity of the same key epitopes of the β-arrestin interface.

Ligand-specific modulation of the conformational spectrum observed at NMR probes supports a role for conformational selection in β-arrestin recruitment. In this model, a preexisting spectrum of conformations is narrowed upon perturbation of the system (*44*), in this case by addition of various ligands. In the ligand-binding pocket, the inactive conformation of $M212^{5x39}$ is a composite of multiple active conformations, suggesting that β-arrestin recruitment is governed not by switching between distinct on and off conformations, but rather by selecting one of many active conformations (active) versus facilitating rapid exchange between them (inactive). The same is only partially true intracellularly: $Met138^{3x46}$ exists as a composite of *trans*/*gauche* rotamers in the inactive state that is narrowed to *gauche*-only rotamers in the active state. Nevertheless, $Met138^{3x46}$ only experiences ring current shift effects in the active state. Although this might suggest that the active-state conformation of $Met138^{3x46}$ is not accessible to ACKR3 in the inactive state, it could also reflect sensitivity limitations of ^{13}C compared with other NMR nuclei (*45*).

How might different ligands enhance or suppress changes in conformational plasticity to regulate β-arrestin? β-arrestin agonists might be described as stabilizing a particular set of conformations that facilitate β-arrestin binding (Fig. 4). Indeed, contact network analysis of inactive- and active-state structures of GPCRs reveals enhanced intermolecular (ligand-residue) and intramolecular (residue-residue) interactions in β-arrestin active states, suggesting that β-arrestin agonists might stabilize specific conformations by organizing denser contact networks. Antagonists fail to fasten these locks, leaving them open (or conformationally heterogeneous), which might disfavor β-arrestin recruitment (Fig. 4).

Whereas NMR data and structural analysis point to the association of β-arrestin recruitment with increased stability, other studies show that G protein activation is associated with conformational heterogeneity at the intracellular region (*46*). There are several possible reasons for this difference. Principally, compared with extensive GPCR–G protein interface (mediated primarily through the α5-helix of G protein), GPCR-β-arrestin interactions are mediated by a smaller, less structured finger loop. Other reasons include dependence of G protein (but not β-arrestin) engagement on outward, destabilizing motions of TM6 (*14*, *25*), and requirement of G protein (but not β-arrestin) coupling to be linked to GTP hydrolysis.

We propose roles for receptor conformations and conformational equilibria in regulating β-arrestin recruitment, but other aspects of β-arrestin coupling must also be considered. For instance, the observed conformational changes might lead to differences in GPCR kinase recruitment between antagonists and agonists, resulting in distinct phosphorylation patterns that alter GPCR functional properties (*47*). Indeed, β-arrestin interaction with phosphorylated GPCRs in the absence of core engagement has been shown to be sufficient for GPCR internalization and β-arrestin–mediated signaling (but not G protein desensitization) (*48*). Nevertheless, other studies have correlated the extent of allosteric coupling between agonists and β-arrestin with a particular ligand's efficacy in β-arrestin recruitment (*49*), suggesting at least some role for GPCR conformational changes dictating β-arrestin engagement.

In summary, our results show that coordinated, allosterically linked changes in receptor dynamics regulate β-arrestin recruitment to the intrinsically biased receptor ACKR3. Our results provide a framework with which to understand the molecular changes required for β-arrestin recruitment and provide insights that may facilitate the design of biased therapeutics.

REFERENCES AND NOTES

1. Y. K. Peterson, L. M. Luttrell, *Pharmacol. Rev.* **69**, 256–297 (2017).
2. D. Wootten, A. Christopoulos, M. Marti-Solano, M. M. Babu, P. M. Sexton, *Nat. Rev. Mol. Cell Biol.* **19**, 638–653 (2018).
3. A. Manglik *et al*., *Nature* **537**, 185–190 (2016).
4. C. L. Schmid *et al*., *Cell* **171**, 1165–1175.e13 (2017).
5. L. M. Slosky *et al*., *Cell* **181**, 1364–1379.e14 (2020).
6. N. K. Singla *et al*., *Pain Pract.* **19**, 715–731 (2019).
7. N. Singla *et al*., *J. Pain Res.* **10**, 2413–2424 (2017).
8. A. S. Hauser, M. M. Attwood, M. Rask-Andersen, H. B. Schiöth, D. E. Gloriam, *Nat. Rev. Drug Discov.* **16**, 829–842 (2017).
9. D. P. Staus *et al*., *Nature* **579**, 297–302 (2020).
10. W. Huang *et al*., *Nature* **579**, 303–308 (2020).
11. Y. Lee *et al*., *Nature* **583**, 862–866 (2020).
12. L. M. Wingler *et al*., *Science* **367**, 888–892 (2020).
13. C. M. Suomivuori *et al*., *Science* **367**, 881–887 (2020).
14. L. M. Wingler *et al*., *Cell* **176**, 468–478.e11 (2019).
15. L. M. Wingler, R. J. Lefkowitz, *Trends Cell Biol.* **30**, 736–747 (2020).
16. C. Wang *et al*., *Science* **340**, 610–614 (2013).
17. S. Rajagopal *et al*., *Proc. Natl. Acad. Sci. U.S.A.* **107**, 628–632 (2010).
18. J. M. Burns *et al*., *J. Exp. Med.* **203**, 2201–2213 (2006).
19. M. Gustavsson *et al*., *Nat. Commun.* **8**, 14135 (2017).
20. M. Meyrath *et al*., *Nat. Commun.* **11**, 3033 (2020).
21. I. R. Kleckner, M. P. Foster, *Biochim. Biophys. Acta* **1814**, 942–968 (2011).
22. A. B. Kleist *et al*., *Methods Cell Biol.* **149**, 259–288 (2019).
23. X. Zhang, R. C. Stevens, F. Xu, *Trends Biochem. Sci.* **40**, 79–87 (2015).
24. R. Sounier *et al*., *Nature* **524**, 375–378 (2015).
25. J. J. Liu, R. Horst, V. Katritch, R. C. Stevens, K. Wüthrich, *Science* **335**, 1106–1110 (2012).
26. V. Isberg *et al*., *Trends Pharmacol. Sci.* **36**, 22–31 (2015).
27. J. D. McCorvy *et al*., *Nat. Struct. Mol. Biol.* **25**, 787–796 (2018).
28. T. Warne, C. G. Tate, *Biochem. Soc. Trans.* **41**, 159–165 (2013).
29. A. J. Venkatakrishnan *et al*., *Nature* **536**, 484–487 (2016).
30. S. G. Rasmussen *et al*., *Nature* **469**, 175–180 (2011).
31. B. F. Volkman, D. Lipson, D. E. Wemmer, D. Kern, *Science* **291**, 2429–2433 (2001).
32. A. S. Solt *et al*., *Nat. Commun.* **8**, 1795 (2017).
33. G. L. Butterfoss *et al*., *J. Biomol. NMR* **48**, 31–47 (2010).
34. Y. Kofuku *et al*., *Nat. Commun.* **3**, 1045 (2012).
35. M. Kayikci *et al*., *Nat. Struct. Mol. Biol.* **25**, 185–194 (2018).
36. M. Szpakowska *et al*., *Br. J. Pharmacol.* **175**, 1419–1438 (2018).
37. R. Nygaard, T. M. Frimurer, B. Holst, M. M. Rosenkilde, T. W. Schwartz, *Trends Pharmacol. Sci.* **30**, 249–259 (2009).
38. R. E. London, B. D. Wingad, G. A. Mueller, *J. Am. Chem. Soc.* **130**, 11097–11105 (2008).
39. S. J. Perkins, K. Wüthrich, *Biochim. Biophys. Acta* **576**, 409–423 (1979).
40. Y. Kang *et al*., *Nature* **523**, 561–567 (2015).
41. G. Fenalti *et al*., *Nature* **506**, 191–196 (2014).
42. V. Katritch *et al*., *Trends Biochem. Sci.* **39**, 233–244 (2014).
43. N. Montpas *et al*., *J. Biol. Chem.* **293**, 893–905 (2018).
44. T. R. Weikl, F. Paul, *Protein Sci.* **23**, 1508–1518 (2014).
45. L. Ye, N. Van Eps, M. Zimmer, O. P. Ernst, R. S. Prosser, *Nature* **533**, 265–268 (2016).
46. A. Manglik *et al*., *Cell* **161**, 1101–1111 (2015).
47. A. Sente *et al*., *Nat. Struct. Mol. Biol.* **25**, 538–545 (2018).
48. T. J. Cahill3rd *et al*., *Proc. Natl. Acad. Sci. U.S.A.* **114**, 2562–2567 (2017).
49. R. T. Strachan *et al*., *J. Biol. Chem.* **289**, 14211–14224 (2014).

ACKNOWLEDGMENTS

We thank A. Dishman for comments on the manuscript and J. Campbell and colleagues at Chemocentryx for supplying CCX777. **Funding:** This work was supported by the National Institutes of Health (grant F30CA196040 to A.B.K.; grant R01AI058072 to B.F.V.; grant F30HL134253 to M.A.T.; grant R35GM133421 to J.D.M.; and grant T32 GM080202 to the Medical Scientist Training Program at Medical College of Wisconsin to A.B.K. and M.A.T.); the State of Wisconsin Tax Check-Off Program for Cancer Research and the Medical College of Wisconsin Cancer Center (B.F.V.); the Luxembourg National Research Fund (Pathfinder "LIH383," INTER/FWO "Nanokine" grant 15/10358798 to A.C.); INTER/FNRS grants 20/15084569, PoC "Megakine" 19/14209621, AFR-3004509, and PRIDE 11012546 "NextImmune" to A.C.; F.R.S.-FNRS-Télévie grants 7.4593.19, 7.4529.19, and 7.8504.20 to A.C.; European Union's Horizon 2020 MSCA Program (grant 641833 ONCORNET and 860229 ONCORNET2.0 to M.J.S.); American Lebanese Syrian Associated Charities (ALSAC grant to M.M.B.); and the UK Medical Research Council (MRC grant MC_U105185859 to M.M.B. and A.S.). **Author contributions:** A.B.K. and B.F.V. conceived of the project. B.F.V. supervised the project. A.B.K. and S.J. made constructs, purified protein, and collected and analyzed NMR data. A.B.K., S.J., and B.F.V. analyzed data, interpreted results, and wrote the manuscript. A.B.K. and S.J. produced the figures. A.B.K. and A.S. performed contact network analysis. A.B.K., A.S., and M.M.B. interpreted contact network analysis data. M.J.S., R.H., and V.B. identified VUN701 and performed nanobody screening and characterization. F.C.P. cloned VUN701, optimized pulse sequences, and oversaw NMR data collection and analysis. M.A.T. made and validated ACKR3 homology model. A.C. identified and provided LIH383 and provided input on binding and functional assays. A.C. and M.S. performed and analyzed fluorescence binding assays and some β-arrestin and binding assays. L.J.L., M.M.C., E.I.A., and L.M.M. performed and G protein and some β-arrestin assays under the supervision of J.D.M.. All authors provided comments on the manuscript. **Competing interests:** B.F.V. and F.C.P. have an ownership interest in Protein Foundry, LLC. R.H. is CSO of QVQ Holding BV. A patent application has been filed on "Novel Selective ACKR3 Modulators and Uses Thereof" (applicant: Luxembourg Institute of Health; inventors: A.C. and M.S.; PCT application no.:

PCT/EP2020/061981). **Data and materials availability:** CCX777 was supplied through a materials transfer agreement (MTA) with Chemocentryx. LIH383 was supplied to B.F.V. through a MTA with A.C. VUN701 was supplied to B.F.V. through a MTA with M.J.S. All data are available in the main text or the supplementary materials. NMR peak assignments are deposited in the Biological Magnetic Resonance Bank (BMRB) under entries 51451 to 51454.

SUPPLEMENTARY MATERIALS

View/request a protocol for this paper from *Bio-protocol*.

Submitted 16 May 2021; accepted 7 June 2022
10.1126/science.abj4922